AD-A256 948

)N PAGE

Form Approved
OMB No 0704-0188

our per response including the time for reviewing instructions searching existing data sources, collection of information. Send comments regarding this burden estimate or any other aspect of this collection of information, including suggestions for reducing this burden to Washington Headquarters Services, Directorate for Information Operations and Reports, 1215 Jefferson Davis Highway, Suite 1204, Arlington VA 22202-4302, and to the Office of Management and Budget, Paperwork Reduction Project (0704-0188), Washington DC 20503.

1. AGENCY USE ONLY (Leave blank)	2. REPORT DATE September 28, 1992	3. REPORT TYPE AND DATES COVERED Final Report 6/1/89-7/31/92

4. TITLE AND SUBTITLE Radiationless transitions and excited-state absorption in tunable laser materials	5. FUNDING NUMBERS DAAL03-89-K-0059

6. AUTHOR(S)

Professor Ralph H. Bartram

7. PERFORMING ORGANIZATION NAME(S) AND ADDRESS(ES) Department of Physics U-46 University of Connecticut Storrs, CT 06269-3046	8. PERFORMING ORGANIZATION REPORT NUMBER

DTIC ELECTE OCT 22 1992 S C D

9. SPONSORING/MONITORING AGENCY NAME(S) AND ADDRESS(ES) U. S. Army Research Office P. O. Box 12211 Research Triangle Park, NC 27709-2211	10. SPONSORING/MONITORING AGENCY REPORT NUMBER ARO 26442.8-PH

11. SUPPLEMENTARY NOTES

The view, opinions and/or findings contained in this report are those of the author(s) and should not be construed as an official Department of the Army position, policy, or decision, unless so designated by other documentation.

12a. DISTRIBUTION/AVAILABILITY STATEMENT Approved for public release; distribution unlimited.	12b. DISTRIBUTION CODE

13. ABSTRACT (Maximum 200 words)

A coordinated experimental and theoretical investigation of fluorescence quenching and excited-state absorption was conducted on the chromium-doped halide elpasolites K_2NaGaF_6, K_2NaScF_6 and Cs_2NaYCl_6, and on the laser-active $Tl^0(1)$ color center in KCl. Luminescence lifetime measurements on $Cs_2NaYCl_6:Cr^{3+}$ revealed a linear pressure dependence of the activation energy for thermal fluorescence quenching which was accurately predicted by a semi-empirical theoretical model incorporating quadratic coupling to an asymmetric mode. An ab-initio theoretical model, based on embedded-cluster and lattice-statics and dynamics calculations, accounted very well for optical and vibrational properties of these materials, but still needs refinement for reliable prediction of thermal quenching behavior. Two-photon excitation spectroscopy helped to explain broad-band excited-state absorption. Embedded-cluster calculations on laser-active color centers are in progress, with encouraging preliminary results.

14. SUBJECT TERMS Non-radiative transitions, transition metals, chromium, tunable lasers, high pressure, luminescence, color centers			15. NUMBER OF PAGES 49
			16. PRICE CODE

17. SECURITY CLASSIFICATION OF REPORT UNCLASSIFIED	18. SECURITY CLASSIFICATION OF THIS PAGE UNCLASSIFIED	19. SECURITY CLASSIFICATION OF ABSTRACT UNCLASSIFIED	20. LIMITATION OF ABSTRACT UL

92-27677

RADIATIONLESS TRANSITIONS AND EXCITED-STATE ABSORPTION IN TUNABLE

LASER MATERIALS

FINAL TECHNICAL REPORT

Ralph H. Bartram

September 28, 1992

U.S. Army Research Office

Contract No. DAAL03-89-K-0059

Department of Physics

University of Connecticut

Storrs, Connecticut 06269-3046

Approved for Public Release;

Distribution Unlimited.

1

THE VIEWS, OPINIONS, AND/OR FINDINGS CONTAINED IN THIS REPORT ARE THOSE OF THE AUTHOR AND SHOULD NOT BE CONSTRUED AS AN OFFICIAL DEPARTMENT OF THE ARMY POSITION, POLICY, OR DECISION, UNLESS SO DESIGNATED BY OTHER DOCUMENTATION.

FOREWORD

The theory of thermally activated radiationless transitions, which compete with luminescence, is well understood in principle, but there is a paucity of examples of its detailed quantitative application to well characterized systems, especially in the intermediate-coupling regime occupied by transition-metal complexes. An analogous situation prevails in the case of excited-state absorption. Athermal fluorescence-quenching mechanisms, which operate in the strong-coupling regime occupied by color centers, are more controversial. The aggressive extension of theory has been made urgently imperative by the exploitation of such systems in potential tunable-laser materials, where fluorescence quenching and excited-state absorption are major loss mechanisms. Low-crystal-field chromium complexes in ordered perovskites of cubic elpasolite structure are a paradigm for vibronic laser materials based on transition-metal doping of ionic crystals. The laser-active $Tl^0(1)$ color center in KCl and its analogues exemplify the strong-coupling regime. The reported investigation has helped to identify factors controlling these important loss mechanisms by detailed experimental characterization of the systems in question and by successful application of semi-empirical models. Ab-initio computer modeling by embedded-molecular-cluster calculations, which require further refinement, may ultimately facilitate formulation of design criteria for such materials.

3

TABLE OF CONTENTS

Page

ILLUSTRATIONS AND TABLES

STATEMENT OF PROBLEM STUDIED

Fluorescence quenching and excited-state absorption are major loss mechanisms in potential tunable-laser materials. The object of the reported investigation was to achieve a quantitative understanding of the factors which control such processes. The ultimate goal is to develop theoretical models with genuine predictive capability, in order to provide guidance in the selection of potential tunable-laser materials by permitting their a-priori evaluation with respect to these loss mechanisms. The subject of the present report on ARO Contract No. DAAL03-89-K-0059 is the completion of an investigation which was initiated under ARO Contract No. DAAG29-82-K-0158 and continued under ARO Contract No. DAAL03-86-K-0017. Experimental techniques employed in this investigation for characterizing low-field chromium complexes and for evaluating radiationless-transition rates include photoluminescence and Raman spectroscopy, at both ambient and high pressures, and two-photon excitation spectroscopy. Radiationless-transition rates were calculated by computer line-shape simulations. A semi-empirical model constrained by spectral information served to identify the dominant photoluminescence quenching mechanism. Ab-initio embedded-molecular-cluster calculations and lattice dynamics calculations were employed in the development of theoretical models with potential predictive capability.

SUMMARY OF RESULTS

I. Introduction

Low crystal-field complexes of Cr^{3+} are characterized by broad-band $(^4T_{2g} \rightarrow {}^4A_{2g})$ fluorescence, in contrast with high-field complexes which exhibit narrow-band $(^2E_g \rightarrow {}^4A_{2g})$ phosphorescence. This property, together with a large Stokes shift, make these low-field complexes ideal candidates for tunable solid-state vibronic laser applications.[1,2,3,4] However, the strong electron-lattice coupling which lends useful properties to these and analogous materials also enhances their susceptibility to both thermal quenching of fluorescence and excited-state absorption, related fundamental processes which proceed from the relaxed excited state of the laser-active center.

The project reported here involved a coordinated experimental and theoretical investigation of thermal fluorescence quenching and excited-state absorption in low-crystal-field chromium complexes in ordered perovskites of cubic elpasolite structure. This class of materials possesses the virtue that a trivalent cation impurity can be accommodated in a rigorously octahedral site without charge compensation. Additionally, it provides chemical sequences with a range of lattice parameters and crystal fields. The specific materials chosen for study include $K_2NaGaF_6:Cr^{3+}$, $K_2NaScF_6:Cr^{3+}$ and $Cs_2NaYCl_6:Cr^{3+}$.

7

Laser-active color centers exhibit even stronger electron-lattice coupling than transition-metal complexes, making them susceptible to an athermal fluorescence quenching mechanism which proceeds from the unrelaxed excited state. The final phase of this investigation included a theoretical investigation of the $Tl^0(1)$ center in KCl and its analogues which is still in progress.

Under the initial contract, No. DAAG29-82-K-0158, fluorescence spectra and lifetimes of chromium-doped elpasolites were measured as functions of temperature in order to parameterize models and to determine activation energies and pre-exponential frequency factors for radiationless-transition rates.[5] A semi-empirical theoretical model was proposed in which radiationless deactivation of the chromium complex is mediated by quadratic coupling to an asymmetric vibrational mode.[6] Photoluminescence spectra of the fluoride elpasolites measured in a diamond-anvil cell revealed a pressure-induced re-ordering of excited states, with a consequent transition from low-field to high-field behavior, and a pressure-induced enhancement of frequencies associated with defect-related vibrational modes.[7,8]

Both experiments and computer modeling were extended during the period of the subsequent contract, No. DAAL03-86-K-0017. Photoluminescence lifetimes in the chloride elpasolite, measured as functions of temperature and pressure in the diamond-anvil

8

cell, revealed a pressure-induced shift of the onset of thermal luminescence quenching to higher temperatures.[9] Ab-initio embedded cluster calculations on the ground electronic state of the chromium complex yielded predictions of the pressure dependence of local compressibility and defect-related vibration frequencies in good accord with experiment. Raman scattering measurements in the diamond-anvil cell provided information about the pressure dependence of both defect-related and host-lattice vibration frequencies.[10,11]

Substantial additional progress in both theory and experiment was made during the period of the contract covered by this report, No. DAAL03-89-K-0059. Photoluminescence spectroscopy was extended to higher pressures and temperatures with the construction of a new diamond-anvil cell, revealing an excited-state level crossing in the chloride elpasolite at higher pressure than in the fluorides, and additional luminescence lifetime measurements on the chloride elpasolite revealed that the pressure dependence of the thermal activation energy for fluorescence quenching is in excellent agreement with predictions of the semi-empirical model.[12,13] Extension of embedded-cluster calculations to the excited state provided optical transition energies in excellent agreement with experiment.[14] Radiationless transition rates predicted by optical line-shape simulations derived from embedded-cluster calculations agreed less well with experiment.[15] Lattice-dynamics calculations provided a good

9

account of Raman spectra[16,17] and of line shapes associated with resolved vibronic structure of emission spectra. Two-photon excitation spectroscopy provided information about electron lattice coupling in a higher excited state.[18] Theoretical models were developed to explain anomalous features of two-photon spectra. Computer modeling of laser-active color centers by ab-initio embedded cluster calculations, initiated during the period of this contract, and is still in progress; preliminary results are encouraging. These developments are elaborated and assessed in the following sections.

II. Thermal Luminescence Quenching Mechanism

There exists an extensive literature on the theory of thermally activated radiationless transitions spanning more than fifty years. In the Mott theory,[19,20] the activation energy for thermal fluorescence quenching is identified with the difference between the crossing energy of the adiabatic potential energy surfaces and the minimum energy of the surface associated with the excited electronic state. The modern, formal development of the theory proceeds from the pioneering contributions of Huang and Rhys[21] and of Lax[22]. Since no radiationless transitions are possible between exact eigenstates of a physical system, the radiationless transition rate depends on the non-stationary state which is prepared in a given experiment, and that in turn depends on the coherence time of the exciting radiation.[23] In the adiabatic

coupling scheme, radiationless transitions are assumed to proceed from Born-Oppenheimer states and are mediated by the non-adiabaticity operator. First-order, time-dependent perturbation theory then leads to an expression for the radiationless transition rate W_{NR} of the form[24]

$$W_{NR} = \nu\omega_p[\bar{n}G(\Omega_0+\omega_p) + (\bar{n}+1)G(\Omega_0-\omega_p)], \tag{1}$$

$$\bar{n} = [\exp(\hbar\omega_p/k_BT) - 1]^{-1}. \tag{2}$$

It is convenient to distinguish between promoting modes, which mix electronic states of different symmetries, and accepting modes, which absorb their energy difference.[25] Coupling to accepting modes is reflected in the normalized line-shape function $G(\Omega)$, where Ω is measured from the zero-phonon line and $\hbar\Omega_0$ is the energy gap to be spanned in the multi-phonon transition. The promoting-mode interaction is incorporated in the factor $\nu\omega_p$, where ω_p is the promoting-mode angular frequency.

Several investigators have demonstrated the equivalence of adiabatic- and static-coupling schemes at a certain level of approximation,[26,27,28,29] and have discredited the popular "Condon approximation" introduced by Huang and Rhys. The static-coupling scheme provides the most tractable formula[30] for ν,

$$\nu = (\pi/\hbar\omega_p^2) \ |\langle\phi(f;0)|\partial H/\partial Q_p|\phi(i;0)\rangle|^2, \tag{3}$$

11

where Q_p is the promoting-mode configuration coordinate.

The central problem in the application of radiationless-transition theory is evaluation of the normalized line-shape function $G(\Omega)$, in Eq. (1), which also describes the wavelength dependence of the fluorescence spectrum for values of its argument Ω which are very far from the range of values accessible to direct observation. The line-shape function is given by

$$G(\Omega) = \sum_{\alpha} P_{\alpha} \sum_{\beta} \prod_{a} |\langle \chi_{f\beta_a} | \chi_{i\alpha_a} \rangle|^2 \; \delta(\Omega_{f\beta} - \Omega_{i\alpha} + \Omega_0 - \Omega), \qquad (4)$$

$$P_{\alpha} = \exp(-\hbar\Omega_{i\alpha}/k_B T) \; / \; \sum_{\gamma} \exp(-\hbar\Omega_{i\gamma}/k_B T), \qquad (5)$$

where $\langle \chi_{f\beta_a} | \chi_{i\alpha_a} \rangle$ is an overlap integral of vibrational wave functions for accepting mode a, associated with final (f) and initial (i) electronic states, with quantum numbers β and α respectively.

Photoluminescence lifetimes of low-field chromium complexes, plotted as functions of temperature, display a characteristic, nearly discontinuous change in slope which signals the onset of thermal quenching. Analysis of lifetime data for the three host crystals studied in the present investigation, $K_2NaGaF_6:Cr^{3+}$,

$K_2NaScF_6:Cr^{3+}$ and $Cs_2NaYCl_6:Cr^{3+}$, yielded thermal-quenching activation energies of 9240, 7270 and 4250 cm^{-1}, respectively, and pre-exponential frequency factors of order 10^{13} sec^{-1}. The measured temperature dependence of photoluminescence spectra served to characterize the chromium complex.

The challenge during the initial phase of this project was to account for the observed thermal-quenching behavior in terms of a semi-empirical theoretical model whose parameters were severely constrained by spectral information. The simple Mott model described above failed by twenty orders of magnitude to explain the observed radiationless transition rate.

In application of the more formal theory encapsulated in Eqs. (1)-(5), a promoting mode of t_{1g} symmetry is required in order to couple the $^4T_{2g}$ excited state with the $^4A_{2g}$ ground state. Counter-rotating displacements of anion octahedra about trivalent and monovalent cations were found to provide a strongly coupled mode of the required symmetry,[31] contrary to earlier speculation concerning promoting-mode selection rules.[32] The promoting-mode factor ν, calculated from Eq. (3) with free-ion chromium d orbitals and the exact nuclear potential for the ligands, is of the order of 10^{15} sec^{-1} for all three host crystals.

It was found that required values of the accepting-mode line-shape function, $G(\Omega_0 \pm \omega_p)$, are extremely sensitive to the precise

physical model adopted for the system when the parameters of the model are constrained by empirical spectral information and by theoretical estimates of the promoting-mode factor ν. Models based on linear coupling to modes of a_{1g} symmetry were found to fail by six to eight orders of magnitude to explain the observed radiationless-transition rate, even when a range of vibration frequencies was considered.

The failure of linear-coupling models suggested consideration of quadratic coupling; i.e., different vibration frequencies in the two electronic states. Although quadratic coupling to a_{1g} modes is possible in principle, it is ruled out in the present system by direct experimental evidence. The octahedral chromium complex has additional degrees of freedom, however, and coupling to lower symmetry accepting modes is permitted by the orbital degeneracy of the $^4T_{2g}$ excited state. In order to limit the number of adjustable parameters, a simplified model was considered which includes just two electronic states, the $^4A_{2g}$ ground state and one orbital component of the $^4T_{2g}$ excited state, with linear coupling to a single a_{1g} accepting mode and quadratic coupling to a single t_{2g} accepting mode. The single a_{1g} accepting mode in this model is an effective mode representing both a_{1g} and e_g modes, which actually have comparable linear coupling. Similarly, the single t_{2g} accepting mode in this model incorporates all of the quadratic coupling which is actually distributed between e_g and t_{2g} modes. Normalized line-shape

14

functions were calculated for each mode by the method of Struck and Fonger,[33] in which individual vibrational overlap integrals are evaluated by the Manneback recursion formula,[34] and the composite line shape was calculated by numerical convolution. Both the a_{1g} and ground-state t_{2g} vibration frequencies were treated as adjustable parameters, but the strength of quadratic coupling was calculated ab initio from a point-ion model. Not only was it possible to fit the temperature dependence of fluorescence spectra and the activation energy for thermal quenching simultaneously, but the model also yielded the correct order of magnitude for the absolute radiationless-transition rate when the estimated value of the promoting mode factor was used. Furthermore, the model worked equally well for all three elpasolite compounds considered, and the adjusted ground-state t_{2g} vibration frequencies are in good agreement with independently determined values.

In the most recent phase of this project, the semi-empirical model was applied successfully to the pressure dependence of thermal fluorescence quenching. A model for thermal fluorescence quenching based on ab-initio embedded cluster calculations was also introduced. These more recent developments are considered in subsequent sections of this report.

III. Pressure Dependence of Chromium Photoluminescence

15

Photoluminescence experiments under intense hydrostatic pressure were initiated to assist in the development and testing of physical models. In the previous phases of this project, photoluminescence spectra and lifetimes of $K_2NaGaF_6:Cr^{3+}$ and $K_2NaScF_6:Cr^{3+}$ were recorded with chopped He-Cd laser excitation at pressures between 0 and 6.5 GPa and at controlled temperatures between 150 and 300 K, by means of a diamond-anvil cell mounted in a cold-finger dewar. In both compounds a transition from low-field to high-field behavior, reflecting a crossing of the $^4T_{2g}$ and ^2E_g excited energy levels, is evidenced by a pronounced blue shift of the featureless fluorescence spectrum and its ultimate replacement by a highly structured phosphorescence spectrum. The interpretation of the vibronic structure of the high-pressure, low-temperature phosphorescence spectra was accomplished by analogy with the ambient-pressure, low-temperature spectrum of the high-field compound $K_2NaAlF_6:Cr^{3+}$, and confirmed by Raman scattering. Vibration frequencies were found to increase by a 2%/GPa in both compounds. The vibronic structure in the scandium compound exhibited an additional feature: the zero-phonon line and each replica were split, providing evidence for a low-temperature phase transition which was subsequently confirmed by both Raman and electron spin resonance spectroscopy.

Photoluminescence spectra of $Cs_2NaYCl_6:Cr^{3+}$ were measured with Ar-ion-laser excitation at pressures between 0 and 11.5 GPa and at controlled temperatures between 80 and 300 K. This compound

exhibits an even more pronounced blue shift than the fluoride compounds and its excited-state level crossing occurs at a much higher pressure (8 GPa, compared with 1 GPa for the gallium compound and 3 GPa for the scandium compound). There is evidence for a pressure-induced phase transition above 9.5 GPa.

The observed blue shift and level crossing in all three compounds is attributed to a substantial pressure-induced enhancement of the crystal-field parameter Dq, associated with reduction of the lattice parameter. A pressure-dependent local compressibility extracted from the measured blue shift of $Cs_2NaYCl_6:Cr^{3+}$ is plotted in Fig. 1.

Luminescence lifetimes of $Cs_2NaYCl_6:Cr^{3+}$ measured as functions of temperature and pressure are plotted in Fig. 2. Excitation was provided by the second harmonic of a Q-switched Nd-YAG laser and signal-averaged data were recorded by a LeCroy fast-transient digitizer. Lifetime data were fit to an expression of the form

$$\tau^{-1} = \tau_0^{-1} \exp(\alpha T) + s \exp[-(\Delta E_0 + \eta P)/k_B T], \qquad (6)$$

where the first term on the right-hand side represents the radiative transition rate and the second term, the non-radiative rate. The parameter values $\tau_0^{-1} = 6370$ sec^{-1}, $\alpha = 0.00403$ K^{-1}, s $= 3.8 \times 10^{13}$ sec^{-1} and $\Delta E_0 = 4250$ cm^{-1} were established at ambient pressure. The activation energy for thermal fluorescence
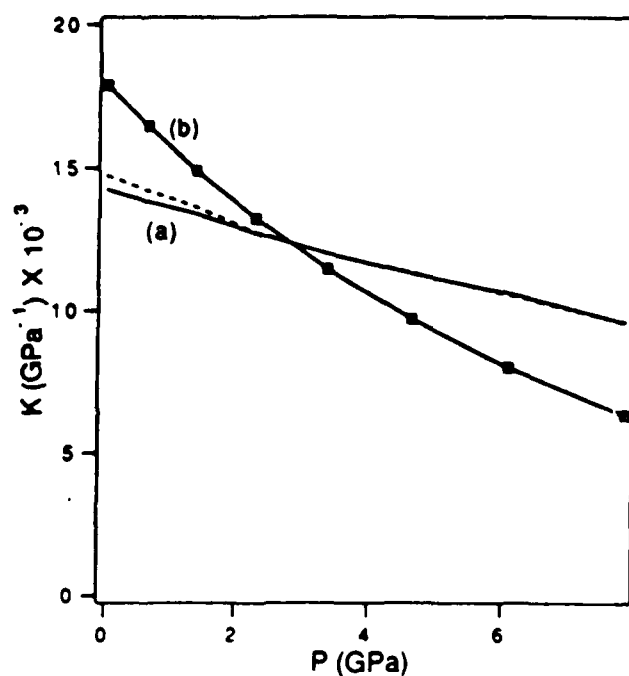
17

Fig. 1. Local compressibility in $Cs_2NaYCl_6:Cr^{3+}$: (a) calculated for ground state (solid line) and first excited state (broken line) and (b) from experimental blue-shift data

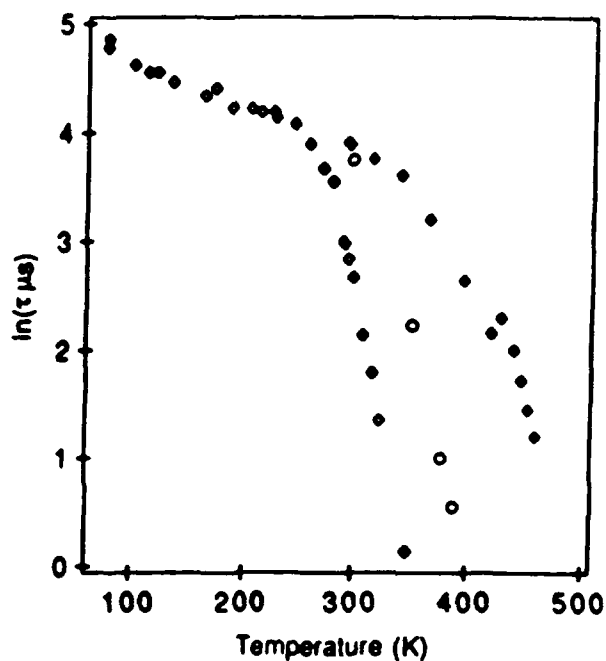Fig. 2. Photoluminescence lifetime τ of $Cs_2NaYCl_6:Cr^{3+}$ vs. temperature at 0 GPa (◇), 0.4 GPa (○) and 1.0 GPa (◆)

quenching was found to depend linearly on pressure with coefficient $\eta = 1668 \pm 52$ cm^{-1}/GPa.

The semi-empirical, two-accepting-mode model described in the preceding section, which incorporates simultaneous linear coupling to an a_{1g} mode and quadratic coupling to a t_{2g} mode, had been devised to explain ambient pressure lifetime data. With the pressure dependence of its parameters derived from that of the photoluminescence spectrum, this model predicts $\eta = 1758$ cm^{-1}/GPa for the pressure dependence of the activation energy in $Cs_2NaYCl_6:Cr^{3+}$, in excellent agreement with experiment.

High-pressure photoluminescence measurements on chromium complexes in elpasolites have proved to be particularly revealing of their properties and processes. Both the pressure-induced re-ordering of excited energy levels and the pressure dependence of thermal quenching are dramatic results which challenge theoretical interpretation. In particular, the latter result provides convincing confirmation of the semi-empirical, two-accepting mode model for thermal fluorescence quenching.

IV. Coherent Raman-Induced Radiationless De-Excitation

At the suggestion of Dr. Mikael Ciftan, an experiment to verify by direct observation the participation of specific accepting modes in the quenching of chromium fluorescence was attempted in

19

collaboration with Professor Walter Bron at the Irvine campus of the University of California. The technique of time-resolved coherent anti-Stokes Raman scattering (TRCARS)[35] was adapted to that purpose. The object of the experiment was to accelerate radiationless de-excitation of substitutional chromium ions in the cubic elpasolite $K_2NaScF_6:Cr^{3+}$ by pulsed excitation of accepting-mode vibrations. Dual synchronously pumped and synchronously amplified mode-locked dye lasers, with their frequency difference tuned to the vibration frequency of the a_{1g} defect mode, effected temporally coherent excitation of that mode. The dye lasers also served to excite the chromium ions to their $^4T_{2g}$ electronic state. The intention was to monitor radiationless de-excitation by detecting anti-Stokes Raman scattering of a delayed probe beam by the accepting-mode vibrations coherently excited in the multi-phonon decay process. The relative amplitudes of the several accepting modes would then indicate the extent of their participation.

Phase matching was irrelevant in this experiment since the impurities lacked translational symmetry; however, the consequent loss of spatial coherence raised the threshold for the desired effect by many orders of magnitude. The minimum energy per pulse required to stimulate radiationless de-excitation was estimated to be 2.5 joules/cm^2, approximately coincident with the laser-damage threshold, as are most other non-linear optical effects involving point defects. Unfortunately, when the experiment was

attempted, laser damage occurred before any evidence of the desired effect could be detected. It was regretfully concluded that the method may be feasible, but not in this material.

V. Computer Modeling of Low-Field Chromium Complexes

Computer modeling of pressure-dependent optical properties by ab-initio embedded-cluster calculations was initiated with the ultimate objective of developing models with genuine predictive capability. Molecular-orbital calculations were performed on a twenty-one atom cluster, $A_8B_6CrX_6^{11+}$, for each compound $A_2BMX_6:Cr^{3+}$, by means of an RHF-LCAO-SCF program called MELD.[36] The 1s, 2s and 2p shells of chromium and its nearest chlorine neighbors were replaced by effective core potentials, while double-ζ quality basis sets for valence orbitals were explicitly included. All nearest-neighbor fluorine orbitals were included, but the nearest sodium and potassium ions were represented by bare effective core potentials.

Interactions of ions inside the cluster with those outside were approximated by central, rigid-ion pair potentials of Buckingham form,

$$V(r) = Z_i Z_j e^2/r + A_{ij} \exp(-r/\rho_{ij}) - C_{ij}/r^6. \tag{7}$$

Simultaneous relaxation of the molecular cluster and its

surrounding lattice was accomplished by means of a modification of the HADESIII lattice statics code,[37] called HADESR, developed under the present project. Electronic structure calculations were performed for both the $^4A_{2g}$ ground state and the $^4T_{2g}$ excited state for each of the compounds of interest. The total energy of the cluster was calculated in each state on a 5x5x5 mesh of symmetrical displacements of X^-, A^+ and B^+ ions surrounding the chromium impurity. This function was fit to a polynomial in symmetry-adapted coordinates and was used to update the total energy and forces at each iteration of the lattice-statics calculation. The calculation then yielded a fully symmetrical relaxed configuration of the crystal, including the embedded cluster, for each electronic state.

Asymmetric displacements were treated more approximately by minimizing the total energy of the $^4T_{2g}$ state with respect to e_g and t_{2g} displacements of X^- ions alone, with the remaining ions fixed in their symmetrically relaxed configuration. The correction for asymmetrical relaxation of the remaining ions was explored at ambient pressure and found to be small.

The total energy of each state was calculated in the relaxed configuration of the other state in order to determine optical transition energies in accordance with the Frank-Condon principle. The effects of pressure were simulated by varying the lattice parameter, which serves as a boundary condition by

22

constraining the ionic configuration at large distances from the impurity.

The predicted $^4T_{2g} \rightarrow {}^4A_{2g}$ optical emission energy of $K_2NaScF_6:Cr^{3+}$ is plotted as a function of pressure in Fig. 3. Also shown for comparison are the peak wavelengths of the broad optical emission bands measured in a diamond-anvil cell. The recorded emission spectra were corrected not only for the response of the detection system, but also for the frequency dependence of the transition probability, in order to facilitate comparison with theory.[38] It is evident that the predicted emission energies are in excellent agreement with experiment.

The predicted $^4A_{2g} \rightarrow {}^4T_{2g}$ optical absorption energy of $K_2NaScF_6:Cr^{3+}$ at ambient pressure, 14,840 cm^{-1}, also compares favorably with the experimental value, 15,601 cm^{-1}. However, the difference between the absorption and emission energies, the Stokes shift, is more sensitive. The calculated value, 1,771 cm^{-1}, increases to 2,045 cm^{-1} when corrected for Jahn-Teller coupling to the t_{2g} mode and for e_g relaxation of the remaining ions outside the octahedron, but it still falls somewhat short of the experimental value, 2,748 cm^{-1}. The corrected Stokes shift predicted for $Cs_2NaYCl_6:Cr^{3+}$, 1,941 cm^{-1}, also falls short of the room-temperature experimental value, 2,642 cm^{-1}, but actually exceeds a reported low-temperature value, 1,740 cm^{-1}.
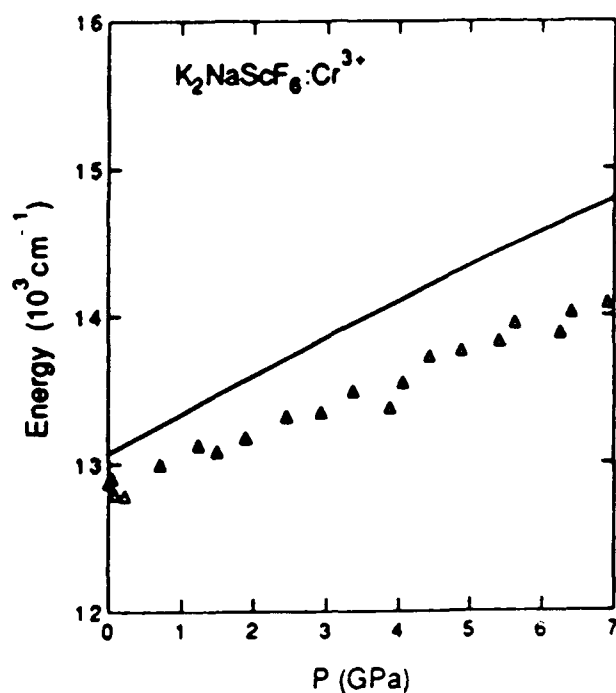
Fig. 3. Pressure dependence of the photoluminescence peak energy for $K_2NaScF_6:Cr^{3+}$. Theory: ———, Experiment: Δ.

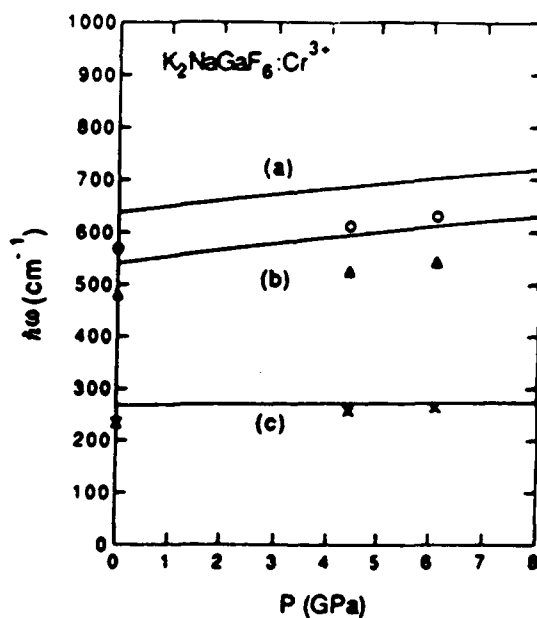Fig. 4. Pressure-dependent ground-state vibration frequencies for $K_2NaGaF_6:Cr^{3+}$. Theory: ———, (a) a_{1g}, (b) e_g and (c) t_{2g}. Experiment: O (a_{1g}), Δ (e_g) and x (t_{2g})

24

Approximate vibration frequencies associated with the chromium impurity were calculated as functions of pressure by exploring the dependence of total energy on a_{1g}, e_g and t_{2g} symmetry-adapted displacements of halogen ions with respect to the relaxed configuration in each electronic state. The calculated pressure dependence of ground-state vibration frequencies of $K_2NaGaF_6:Cr^{3+}$ is compared with values inferred from resolved vibronic structure of emission spectra in Fig. 4. Calculated vibration frequencies exceed experimental values by $\approx$ 15 % in all three compounds; this systematic discrepancy is attributed in part to neglect of electron correlation.

A new method was developed for optical line-shape simulation by direct diagonalization of the matrix of the vibrational Hamiltonian within each electronic state in a common harmonic oscillator basis. The vibrational overlap integrals in Eq. (4) were evaluated as the direct products of eigenvectors, and the corresponding energy eigenvalues were employed in evaluating the delta-function factors. This method accurately replicates line shapes for combined linear and quadratic coupling which were calculated previously by the Manneback recursion relations. However, the new method is much more general in that it can also accommodate any form of anharmonicity for which the matrix elements can be calculated; i.e., any which is expressible as a power series in the configuration coordinate.

25

The new method was applied to calculation of radiationless transition rates between $^4T_{2g}$ and $^4A_{2g}$ states of the chromium-doped elpasolites K_2NaGaF_6, K_2NaScF_6 and Cs_2NaYCl_6. Adiabatic potential energy surfaces for each electronic state were derived from the ab-initio embedded cluster calculations described previously. The 5x5x5 mesh provided not only linear and quadratic coupling to a_{1g} modes, but also cubic and quartic anharmonic coupling. Only linear and quadratic coupling to e_g and t_{2g} modes was considered, except for the chloride compound, where anharmonic coupling to a t_{2g} mode was investigated by means of configuration-interaction (CI) calculations.

Radiationless transition rates predicted for $K_2NaScF_6:Cr^{3+}$ are compared with experiment in Fig. 5. Rates predicted for the fluoride compounds in the harmonic approximation were lower by two orders of magnitude than the values inferred from experiment; equivalently, the temperature predicted for the onset of luminescence quenching was too high by a factor of two. This result is a substantial improvement on the single-configuration-coordinate, linear-coupling model with parameters constrained by empirical spectral information, which fails by seven orders of magnitude. The predicted transition rate for the chloride compound, on the other hand, was too small by ten orders of magnitude, essentially because the anticipated quadratic coupling to the t_{2g} mode failed to materialize in that case. Inclusion of a_{1g} anharmonicity worsened the agreement in all three compounds.
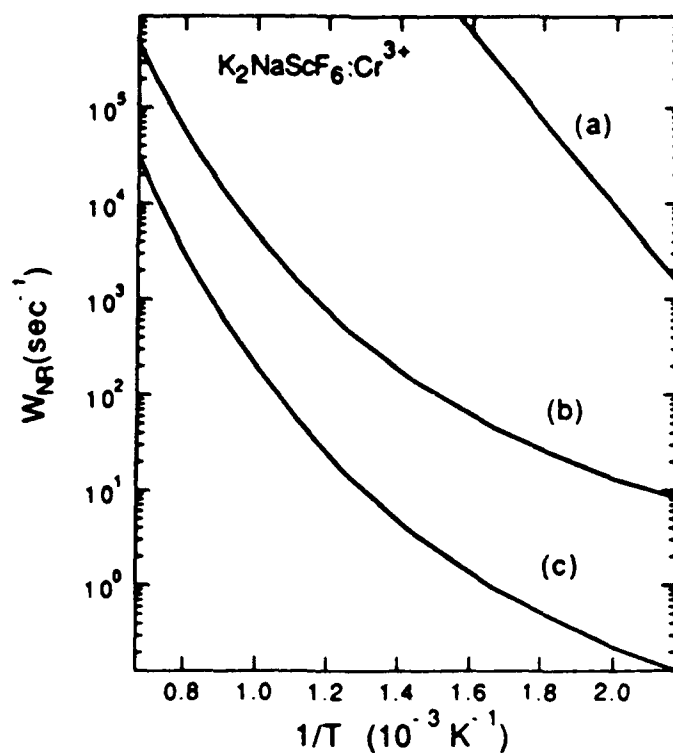
26

Fig. 5. Radiationless rate $W_{NR}(T)$ for $K_2NaScF_6:Cr^{3+}$ at P = 0: (a) Experiment, (b) Harmonic theory and (c) Anharmonic theory
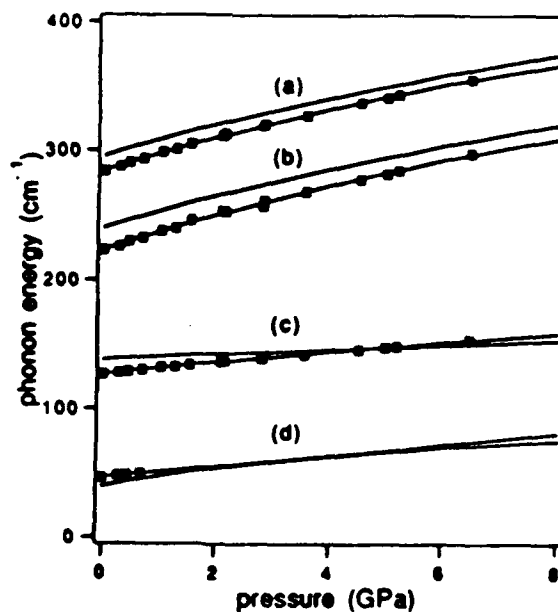

Fig. 6. Calculated (———) and measured Raman frequencies of Cs_2NaYCl_6 vs. pressure: (a) a_{1g}, (b) e_g, (c) $t_{2g}^{(2)}$ and (d) $t_{2g}^{(1)}$

27

VI. Lattice Dynamics Calculations

Host-lattice vibration frequencies were calculated as functions of wave vector from the same phenomenological pair potentials employed in lattice-statics calculations. This investigation led to a re-evaluation of the pair potentials subsequently employed in embedded cluster calculations. Revised pair potentials incorporate theoretically determined Van der Waals coefficients and a slightly reduced ($<$ 5 %) Born-Mayer parameter ρ adjusted to fit solid-state properties at ambient pressure.

The frequencies of Raman-active modes at zone-center were calculated as functions of hydrostatic pressure. Calculated frequencies for Cs_2NaYCl_6 are compared with experimental values inferred from Raman spectra in Fig. 6.

Vibration frequencies were calculated along symmetry directions in the first Brillouin zone at ambient pressure, yielding phonon dispersion curves. An imaginary frequency associated with a t_{1g} displacement explains the low-temperature phase transition observed in K_2NaScF_6.

Frequencies were also calculated as functions of pressure on a Kellerman mesh in the first Brillouin zone, yielding the phonon density of states and frequency-dependent perfect-lattice Green's function matrix elements for symmetry-adapted displacements of

28

the six fluorine neighbors of a trivalent cation. The latter were employed in conjunction with force-constant changes derived from embedded cluster calculations on the chromium impurity to construct defect-lattice Green's function matrix elements. The predicted density of normal modes projected on halogen displacements is consistent with the narrow vibrational sidebands in optical spectra which are conventionally attributed to normal modes of the chromium hexahalide octahedron.[39]

VII. Two-Photon Excitation Spectroscopy

Two-photon excitation spectroscopy at low temperature, employed previously in transition-metal complexes by McClure and co-workers,[40] has the virtue that two-photon transitions between electronic states of the same parity are electric-dipole allowed, whereas one-photon transitions are forbidden. Consequently, the vibronic structure of the two-photon spectrum is greatly simplified, since progressions of even-mode phonon replicas are built on a prominent zero-phonon line rather than on false origins associated with odd modes. The object of the investigation reported here was to characterize the electron-lattice coupling in a higher excited state of $K_2NaScF_6:Cr^{3+}$ in order to achieve a better understanding of excited-state absorption (ESA). In particular, it is important to account for the exceptional width of ESA bands in transition-metal complexes, which makes them so deleterious to laser operation. Experiments

were performed on an oriented single crystal at low temperatures (4-10 K) with Raman-shifted, Nd:YAG-pumped dye-laser excitation. Two-photon absorption (TPA) was monitored by photomultiplier detection of polarized chromium fluorescence.

The $^4A_{2g} \rightarrow {}^4T_{1ga}$ TPA transition was emphasized in the present investigation. The corresponding ESA band, $^4T_{2g} \rightarrow {}^4T_{1ga}$, overlaps only a small portion of the tuning range of a potential tunable laser based on this material. However, the more important $^4T_{1gb}$ state is inaccessible by the present technique because its TPA spectrum overlaps the one-photon $^4A_{2g} \rightarrow {}^4T_{2g}$ excitation spectrum for chromium fluorescence.

A well-resolved two-component zero-phonon line was observed whose splitting was attributed to the established low-temperature phase transition in this material; spin-orbit splitting is evidently suppressed by strong Jahn-Teller coupling. Convolved line-shape simulations established equal coupling to a_{1g} and e_g modes in the $^4T_{1ga}$ state, comparable in strength to that for the $^4T_{2g}$ state, plus much stronger coupling to the t_{2g} mode, which is virtually absent in the $^4T_{2g}$ state. The latter coupling, together with opposing displacements of the e_g coordinate in the two states, accounts very well for the width of the excited-state absorption spectrum.

Additional features encountered in the $^4A_{2g} \rightarrow {}^4T_{1ga}$ TPA spectrum

30

include anomalous polarization anisotropy of the broad vibronic sideband, relative to that of the zero-phonon line, and anomalously extended progressions of phonon replicas. The former feature was explained in terms of departures from the crude Born-Oppenheimer approximation induced by strong coupling to the t_{2g} mode. The latter feature, which had been observed previously in another material, was explained by the coupling of intermediate states with diffuse wavefunctions to lattice modes involving displacements of more remote ions.

The $^4A_{2g} \rightarrow {}^4T_{2g}$ TPA spectrum was also observed, in spite of the fact that this transition is forbidden by two-photon selection rules.[41] No zero-phonon line was observed, and it finally became apparent that the entire spectrum consisted of progressions built on a false e_g origin. Lineshape simulations supported equal coupling to a_{1g} and e_g modes, in confirmation of one-phonon spectra, and negligable coupling to the t_{2g} mode. Neither anomalous polarization anisotropy nor anomalously extended progressions were observed. However, the broad sideband was perturbed by Fano anti-resonances associated with ^2E_g and $^2T_{1g}$ multiplicity-forbidden TPA transitions.

VIII. Computer Modeling of Laser-Active Color Centers

Vibronic lasers based on color centers in ionic crystals are emerging as serious candidates for long-wavelength sources in

31

telecommunications. However, their very strong electron-lattice coupling makes them susceptible to an additional, athermal fluorescence quenching mechanism. This quenching mechanism, which operates during the relaxation process at T = 0, was first identified by Dexter, Klick and Russell (DKR)[42] and was subsequently elaborated by Bartram and Stoneham[43] and others. The DKR rule predicts radiationless de-excitation of color centers when the excited-state energy reached in a Frank-Condon transition from the ground state lies above the intersection of adiabatic potential energy curves. For linear coupling, this criterion corresponds to $\Lambda > 0.25$, where Λ is defined as the ratio of the excited-state lattice relaxation energy to the optical absorption energy.

The $Tl^0(1)$ center in alkali halides, produced by subjecting a thallium-doped crystal to ionizing radiation and consisting of a substitutional neutral thallium atom adjacent to an anion vacancy,[44] has proved to be one of the most promising laser-active color centers.[45] The electronic and vibronic structure of this center were investigated in some detail by multiple resonance techniques.[46] The analogous $Ga^0(1)$ and $In^0(1)$ centers in KCl, however, exhibited little or no luminescence even at a temperature of 10 K. It was demonstrated by a model calculation that the disparate behavior of these analogous centers could be explained in terms of the DKR quenching mechanism, and that the parameter which distinguishes them is their spin-orbit coupling.[47]

This analysis led to the prediction that the analogous $Pb^+(1)$ center in halides with divalent cations should exhibit efficient luminescence, at least by the DKR criterion. That prediction has since been corroborated for Pb-doped, X-irradiated alkaline-earth fluorides,[48] where laser action is inhibited by excited-state absorption,[49] and lasing was demonstrated in X-irradiated, Pb-doped $KMgF_3$ which is probably attributable to this center.[50]

Ab-initio embedded cluster calculations on $Tl^0(1)$ centers were initiated as part of the present project. A double-ζ quality basis set with effective core potentials for the thallium atom and its nearest chlorine neighbor opposite the vacancy was augmented by diffuse vacancy-centered orbitals derived from an independent F-center calculation. The remaining ions in the 44-ion cluster were represented by bare effective core potentials. RHF-SCF-LCAO molecular-orbital calculations were performed on the ground state and lowest excited state by means of the MELD program.

The spin-orbit splitting Δ was reduced from that of the free thallium atom by the fraction of thallium p orbital in the open-shell molecular orbital. The energies of the three lowest states were then approximated as follows:

$$W_{2,1} = \frac{\Delta - \gamma}{2} \pm \frac{1}{2} \sqrt{(\Delta - \gamma)^2 + 8\gamma^2} + E_0, \qquad (8)$$

33

$$W_3 = \Delta + \gamma + E_0, \tag{9}$$

$$E_0 = \frac{E_g + 2E_e}{3}, \tag{10}$$

$$\gamma = \frac{E_e - E_g}{3} + \gamma_0, \tag{11}$$

where E_g and E_e are, respectively, the energies of the non-degenerate ground state and the doubly-degenerate lowest excited state, obtained from molecular-orbital calculations in the absence of spin-orbit interaction. The parameter γ_0 was introduced to correct for the difference between the axial chlorine neighbor with valence orbitals and the transverse chlorine neighbors represented by effective core potentials.

Molecular-orbital calculations were performed for various combinations of axial thallium displacements and four symmetry-adapted displacements of the immediate neighbors of the thallium atom and chlorine vacancy. Simultaneous relaxation of the embedded cluster and surrounding lattice was accomplished by the HADESR program. Optical transition energies and the ground-state thallium vibration frequency are compared with experiment[51,52] in Table 1.

Table 1. Predicted and measured optical transition energies and thallium vibration frequency of the $Tl^0(1)$ center in KCl

	E_{abs} (eV)	E_{em} (eV)	ω (10^{13} sec^{-1})
Theory	1.38	0.98	0.77
Experiment	1.20	0.83	0.57

Adiabatic potential energy functions generated in this type of calculation will ultimately provide the basis for a theoretical investigation of the athermal luminescence quenching behavior of inactive $Ga^0(1)$ and $In^0(1)$ analogues, and thus for a prediction of their residual quantum efficiency of fluorescence.

IX. Summary and Conclusions

Radiationless transitions generally belong to one of two categories: static processes which are thermally activated from a metastable state, and dynamic processes which occur during rapid relaxation immediately following excitation. Both categories were of interest in the context of the present investigation of luminescence quenching, the former for chromium complexes and the latter for color centers.

The chromium-doped elpasolite crystals selected for this investigation provided a chemical sequence of low-field chromium complexes, with rigorous octahedral site symmetry, typical of

transition-metal based tunable laser materials. The range of crystal-field parameters was further extended by application of hydrostatic pressure, culminating in the crossing of excited-state energy levels. Detailed characterization of these materials was accomplished by one- and two-photon optical absorption spectroscopy, pressure-dependent photoluminescence and Raman spectroscopy and electron paramagnetic resonance spectroscopy. Photoluminescence lifetime data as functions of temperature and pressure provided a measure of thermal fluorescence quenching, and the temperature and pressure dependence of photoluminescence spectra served to constrain the parameters of various electron-lattice coupling models.

A semi-empirical, two-accepting-mode model, devised to explain photoluminescence lifetime data at ambient pressure, proved to be extremely successful in predicting the observed pressure dependence of the activation energy for thermal fluorescence quenching as well. Although the semi-empirical model is known to be oversimplified, this successful prediction appears to confirm its essential features: the dependence of the quenching mechanism on quadratic coupling and on coupling to asymmetric modes.

An *ab-initio* three-accepting-mode model, based on RHF-LCAO-SCF embedded cluster calculations with static lattice relaxation, predicts pressure-dependent optical transition energies in excellent agreement with experiment in all three compounds. The

36

predicted ambient-pressure Stokes shifts are systematically 30 % lower than experimental values measured at room temperature; however, that for the chloride compound is 10 % higher than a reported low-temperature value. Predicted pressure-dependent defect-related vibration frequencies are systematically high by about 15 %. Finally, predicted radiationless transition rates are low by two orders of magnitude in the fluoride compounds, or, equivalently, the predicted temperature for the onset of thermal quenching is too high by a factor of two. This result is a substantial improvement on the single-configuration-coordinate, linear-coupling model with parameters constrained by empirical spectral information, which fails by seven orders of magnitude. However, the predicted rate for the chloride compound is too low by ten orders of magnitude. Anharmonicity worsened the agreement in all cases.

Both the semi-empirical model and the ab-initio model developed in this project go far beyond what has been attempted previously in the theory of radiationless transitions. Models incorporating linear and/or quadratic coupling to a single, symmetrical mode have been reported, but they have invariably incorporated adjustable parameters whose adjusted values are grossly incompatible with the optical properties of the system in question. A proposed explanation of high radiationless transition rates based on anharmonic coupling,[53] which is widely accepted, has been shown to be inapplicable in the present case.

37

The semi-empirical model served to identify the controlling mechanism for radiationless de-activation of the chromium complexes under investigation. The ab-initio model, on the other hand, still falls short of the kind of predictive capability required for tunable-laser design applications, although it represents a giant step in that direction.

An obvious refinement of the ab-initio embedded-cluster model would be the addition of configuration interaction (CI) at the level of single and double excitations selected by diagrammatic perturbation theory. The principal difference in treatment of the chloride compound and the fluoride compounds was the use of an effective core potential for the chloride ion and an all-electron calculation for the fluoride ion; the all-electron representation of the chloride ion is feasible as well, but pushes computing-time limits. Even with these refinements, however, the model as presently formulated would be incapable of predicting the observed temperature dependence of the Stokes shift, which is related to both thermal expansion and quadratic coupling. The model portrays the lattice as too rigid at the elevated temperatures where radiationless transitions actually occur, and thus underestimates the electron-lattice coupling on which the transition rate depends very sensitively. In principle, lattice relaxation at a finite temperature should minimize the total Gibbs free energy rather than the total internal energy. It remains to incorporate such a refinement in

38

the basic lattice-statics algorithm.

Lattice dynamics calculations served to demonstrate that the same pair potentials employed in the lattice-statics calculations could explain pressure-dependent Raman scattering data as well. They also confirmed the assignment of resolved vibronic structure of emission spectra to modes of the chromium hexahalide octahedron, and thus validated the more approximate method of calculating vibration frequencies.

Two-photon excitation spectroscopy revealed strong Jahn-Teller coupling to t_{2g} modes in the $^4T_{1ga}$ state which is absent in the $^4T_{2g}$ state, thus elucidating the origin of the exceptional width of the $^4T_{2g} \rightarrow {}^4T_{1ga}$ excited-state absorption band. Unexpected and theoretically challenging features of the TPA spectra included anomalous polarization anisotropy, anomalously extended progressions and forbidden transitions.

Preliminary embedded-cluster calculations with static lattice relaxation performed on low-symmetry laser-active color centers successfully predicted optical transition energies and a Raman frequency. These calculations are ultimately directed toward an in-depth investigation of dynamic radiationless transitions which impede laser action in analogous centers.

PUBLICATIONS

All publications which appeared in print during the period of the present contract, DAAL03-89-K-0059, and presentations which were made during that period are listed below for completeness, although some of them are attributable to previous contracts. The list remains incomplete, however, since several additional manuscripts and one thesis are still in preparation.

A.   Journal Articles and Proceedings

1.   R.H. Bartram, "Radiationless transitions of point imperfections in solids", *J. Phys. Chem. Solids* **51**, 641-651 (1990) (invited review article)

2.   U. Sliwczuk, R.H. Bartram, D.R. Gabbe and B.C. McCollum, "Raman scattering of chromium-doped halide elpasolite crystals", *J. Phys. Chem. Solids* **52**, 357-361 (1991)

3.   U. Sliwczuk, A.G. Rinzler, L.A. Kappers and R.H. Bartram, "Pressure dependence of Raman scattering by chromium-doped halide elpasolite crystals", *J. Phys. Chem. Solids* **52**, 363-365 (1991)

4.   J.-M. Spaeth, R.H. Bartram, M. Rac and M. Fockele, "Upconversion by excited state absorption of $Pb^+(1)$ centres in alkaline-earth fluorides. *J. Phys.:Condens. Matter* **3**, 5013-5022 (1991)

5. R.H. Bartram, A.M. Woods, R.S. Sinkovits, J.C. Charpie and A.R. Rossi, "Embedded cluster modeling of excited chromium impurities in halide elpasolites", *Radiation Effects and Defects in Solids* 119-121, 627-632 (1991)

6. R.S. Sinkovits and R.H. Bartram, "Computer modeling of lattice dynamics in halide elpasolites", *J. Phys. Chem. Solids* 52, 1137-1144 (1991)

7. J.F. Dolan, A.G. Rinzler, L.A. Kappers and R.H. Bartram, "Pressure and temperature dependence of chromium photoluminescence spectra in fluoride elpasolites", *J. Phys. Chem. Solids* 53, 905-912 (1992)

8. A.G. Rinzler, J.F. Dolan, L.A. Kappers, D.S. Hamilton and R.H. Bartram, "Pressure dependence and thermal quenching of chromium photoluminescence in $Cs_2NaYCl_6:Cr^{3+}$", *J. Phys. Chem. Solids* (in press)

9. R.H. Bartram, A.G. Rinzler, J.F. Dolan, A.M. Woods, R.S. Sinkovits, L.A. Kappers and D.S. Hamilton, "Measured and predicted pressure-dependent radiationless transition rates in chromium-doped halide elpasolites", *Proceedings of the International Conference on Defects in Insulating Materials*, Nordkirchen, Germany, August 22-26, 1992 (in press)

10. R.H. Bartram and T.J. Gryk, "Embedded cluster modeling of the $Tl^0(1)$ center in KCl", *Proceedings of the International Conference on Defects in Insulating Materials*, Nordkirchen, Germany, August 22-26, 1992 (in press)

11. A.M. Woods, R.S. Sinkovits, J.C. Charpie, W.L. Huang, R.H. Bartram and A.R. Rossi, "Computer modeling of the optical properties of chromium-doped halide elpasolites" (to be submitted for publication)

B. Theses

1. Robert S. Sinkovits, *Computational modeling of lattice statics and dynamics in crystals of the elpasolite structure*, doctoral dissertation, University of Connecticut, 1991

2. Amanda M. Woods, *Molecular cluster modeling of chromium complexes in elpasolite crystals*, doctoral dissertation, University of Connecticut, 1991

3. Andrew G. Rinzler, *Optical studies at high pressure on chromium-doped ordered perovskite crystals*, doctoral dissertation, University of Connecticut, 1991

4. George Robert Wein, *Two-photon excitation spectroscopy of $Cr^{3+}:K_2NaScF_6$*, doctoral dissertation, University of Connecticut, 1992

C. Presentations at Meetings

1. R.H. Bartram, "Molecular cluster modeling of point imperfections in crystals", Symposium on Physics of Optical Crystals, Budapest, Hungary, October 10-12, 1989 (invited paper)

2. R.S. Sinkovits and R.H. Bartram, "Computer modeling of lattice dynamics in halide elpasolites", *Bull. Am. Phys. Soc.* **35**, 356 (1990)

3. A.M. Woods, R.S. Sinkovits, J.C. Charpie, R.H. Bartram and A.R. Rossi, "Computer modeling of chromium ions in halide elpasolites", *Bull. Am. Phys. Soc.* **35**, 691 (1990)

4. A.G. Rinzler, L.A. Kappers, R.H. Bartram and J.F. Dolan, "Pressure-dependent photoluminescence spectroscopy of a chromium-doped chloride elpasolite crystal", XVII International Quantum Electronics Conference, Anaheim, California, May 21-25 (1990)

5. R.H. Bartram, A.M. Woods, R.S. Sinkovits, J.C. Charpie and A.R. Rossi, "Embedded cluster modeling of excited chromium impurities in halide elpasolites", Sixth Europhysical Topical Conference: Lattice Defects in Ionic Materials, Groningen, The Netherlands, September 3-7, 1990

6. A.M. Woods, R.S. Sinkovits and R.H. Bartram, "Predicted non-radiative transition rates in chromium-doped halide elpasolites", *Bull. Am. Phys. Soc.* **36**, 891 (1991)

7. R.S. Sinkovits, A.M. Woods and R.H. Bartram, "Emission lineshapes of chromium-doped halide elpasolites", *Bull. Am. Phys. Soc.* **36**, 892 (1991)

8. G.R. Wein, D.S. Hamilton and R.H. Bartram, "Polarization anisotropy in two-photon excitation spectra of $K_2NaScF_6:Cr^{3+}$", *Bull. Am. Phys. Soc.* **36**, 892 (1991)

9. G.R. Wein, D.S. Hamilton and R.H. Bartram, "Polarization anisotropy of extended vibrational structure in two-photon absorption", Quantum Electronics-Laser Science (QELS) Conference, Baltimore, MD, May 12-17, 1991

10. R.H. Bartram, A.G. Rinzler, J.F. Dolan, A.M. Woods, R.S. Sinkovits, L.A. Kappers and D.S. Hamilton, "Measured and predicted pressure-dependent radiationless transition rates in chromium-doped halide elpasolites", International Conference on Defects in Insulating Materials, Nordkirchen, Germany, August 22-26, 1992

11. R.H. Bartram and T.J. Gryk, "Embedded cluster modeling of the $Tl^0(1)$ center in KCl", International Conference on Defects in Insulating Materials, Nordkirchen, Germany, August 22-26, 1992

SCIENTIFIC PERSONNEL

A. Senior Personnel Supported

    1. Professor Ralph H. Bartram (Principal Investigator)

    2. Associate Professor Lawrence Kappers

B. Graduate Students Supported

    1. Wen-Li Huang

    2. Andrew G. Rinzler

    3. Robert S. Sinkovits

    4. Amanda M. Woods

    5. George Robert Wein

C. Unsupported Research Collaborators

    1. Professor Douglas Hamilton

    2. Dr. Angelo Rossi (IBM)

    3. Postdoctoral Fellow Uwe Sliwczuk (Physics, U. Conn.)

    4. Prof. Dr. J.-M. Spaeth (Uni. Paderborn, Germany)

    5. Professor Walter Bron (U. Cal. Irvine)

    6. Graduate Student Thomas Gryk

BIBLIOGRAPHY

[1]J.C. Walling, O.G. Peterson, H.P. Jensen, R.C. Morris and E.W. O'Dell, *IEEE J. Quantum Electron.* QE-16, 1302 (1980)

[2]J. Buchert and R.R. Alfano, *Laser Focus* 19, 117 (1983)

[3]M.L. Shand and J.C. Walling, *IEEE J. Quantum Electron.* QE-18, 1829 (1982)

[4]B. Struve, G. Huber, V.V. Lapter, I.A. Scherbakov and Y.V. Zharikov, *Appl. Physics B* 28, 235 (1982)

[5]L.J. Andrews, A. Lempicki, B.C. McCollum, C.J. Giunta, R.H. Bartram and J.F. Dolan, *Phys. Rev. B* 34, 2735 (1986)

[6]R.H. Bartram, J.C. Charpie, L.J. Andrews and A. Lempicki, *Phys. Rev. B* 34, 2741 (1986)

[7]J.F. Dolan, L.A. Kappers and R.H. Bartram, *Phys. Rev. B* 33, 7339 (1986)

[8]J.F. Dolan, A.G. Rinzler, L.A. Kappers and R.H. Bartram, *J. Phys. Chem. Solids* 53, 905 (1992)

[9]R.H. Bartram, J.F. Dolan, J.C. Charpie, A.G. Rinzler and L.A. Kappers, *Cryst. Latt. Def. and Amorph. Mat.* 15, 165 (1987)

[10]U. Sliwczuk, R.H. Bartram, D.R. Gabbe and B.C. McCollum, *J. Phys. Chem. Solids* 52, 357 (1991)

[11]U. Sliwczuk, A.G. Rinzler, L.A. Kappers and R.H. Bartram, *J. Phys. Chem. Solids* 52, 363 (1991)

[12]A.G. Rinzler, *Optical studies at high pressure on chromium-doped ordered perovskite crystals*, Ph.D. dissertation, U. Conn. (1991)

[13]A.G. Rinzler, J.F. Dolan, L.A. Kappers, D.S. Hamilton and R.H. Bartram, *J. Phys. Chem. Solids* (in press)

[14]R.H. Bartram, A.M. Woods, R.S. Sinkovits, J.C. Charpie and A.R. Rossi, *Radiation Effects and Defects in Solids* 119-121, 627 (1991)

[15]A.M. Woods, *Molecular cluster modeling of chromium complexes in elpasolite crystals*, Ph.D. dissertation, U. Conn. (1991)

[16]R.S. Sinkovits and R.H. Bartram, *J. Phys. Chem. Solids* 52, 1137 (1991)

[17]R.S. Sinkovits, *Computational modeling of lattice statics and dynamics in crystals of the elpasolite structure*, Ph.D. dissertation, U. Conn. (1991)

[18]G.R. Wein, *Two-photon excitation spectroscopy of* $Cr^{3+}:K_2NaScF_6$, Ph.D. dissertation, U. Conn. (1992)

[19]N.F. Mott, *Proc. R. Soc. London A* 167, 384 (1938)

[20]R.W. Gurney and N.F. Mott, *Trans. Faraday Soc.* 35, 69 (1939)

[21]K. Huang and R. Rhys, *Proc. R. Soc. London A* 203, 406 (1950)

[22]M. Lax, *J. Chem. Phys.* 20, 1752 (1952)

[23]W. Rhodes, *Chem. Phys.* 22, 95 (1977)

[24]R.H. Bartram, *J. Phys. Chem. Solids* 51, 641 (1990)

[25]S.H. Lin and R. Bersohn, *J. Chem. Phys.* 48, 2732 (1968)

[26]G. Helmis, *Ann. Physik* 19, 41 (1956)

[27]R. Pässler, *Czech. J. Phys. B* 24, 322 (1974)

[28]K. Huang, *Scientia Sinica* 24, 27 (1981)

[29]E. Gutsche, *Phys. Stat. Sol. (b)* 109, 583 (1982)

[30] R.H. Bartram and A.M. Stoneham, *J. Phys. C:Solid State Phys.* 18, L549 (1985)

[31] A. Lentz, *J. Phys. Chem. Solids* 35, 827 (1974)

[32] L.J. Andrews, A. Lempicki and B.C. McCollum, *Chem. Phys. Lett.* 74, 404 (1980)

[33] C.W. Struck and W.H. Fonger, *J. Luminescence* 10, 1 (1975)

[34] C. Manneback, *Physica* 17, 1001 (1951)

[35] W.E. Bron, J. Kuhl and B.K. Rhee, *Phys. Rev. B* 34, 6961 (1986)

[36] E.R. Davidson et al., MELD, Quantum Chemistry Group, University of Washington

[37] A.B. Lidiard and M.J. Norgett, in *Computational Solid State Physics*, Eds. F. Herman, N.W. Dalton and T.R. Koehler (Plenum, NY, 1978) pp. 385-412

[38] A.J. Wojtowicz, M. Kazmierczak, A. Lempicki and R.H. Bartram, *J. Opt. Soc. Am. B* 6, 1106 (1989)

[39] P. Greenough and A.G. Paulusz, *J. Chem. Phys.* 70, 1967 (1979)

[40] R.-L. Chien, J.M. Berg, D.S. McClure, P. Rabinowitz and B.N. Perry, *J. Chem. Phys.* 84, 4168 (1986)

[41] T.R. Bader and A. Gold, *Phys. Rev.* 171, 997 (1968)

[42] D.L. Dexter, C.C. Klick and G.A. Russell, *Phys. Rev.* 100, 603 (1955)

[43] R.H. Bartram and A.M. Stoneham, *Solid St. Commun.* 17, 1593 (1975)

[44] E. Goovaerts, J. Andriessen, S.V. Nistor and D. Schoemaker, *Phys. Rev.B* 24, 29 (1981)

[45]W. Gellerman, F. Luty and C.R. Pollock, *Optics Comm.* **39**, 391 (1981)

[46]F.J. Ahlers, F. Lohse, J.-M. Spaeth and L.F. Mollenauer, *Phys. Rev. B* **28**, 1249 (1983)

[47]F.J. Ahlers, F. Lohse, Th. Hangleiter, J.-M. Spaeth and R.H. Bartram, *J. Phys. C:Solid State Phys.* **18**, 1963 (1984)

[48]M. Fockele, F. Lohse, J.-M. Spaeth and R.H. Bartram, *J. Phys.: Condens. Matter* **1**, 13 (1989)

[49]J.-M. Spaeth, R.H. Bartram, M. Rac and M. Fockele, *J. Phys. Condens. Matter* **3**, 5013 (1991)

[50]G. Horsch and H.J. Paus, *Opt.Comm.* **60**, 69 (1987)

[51]L.F. Mollenauer , N.D. Vieira and L. Szeto, *Phys. Rev. B* **24**, 29 (1983)

[52]W. Joosen, E. Goovaerts and D. Schoemaker, *Phys. Rev. B* **32**, 6748 (1985)

[53]M.D. Sturge, *Phys. Rev. B* **8**, 6 (1973)